Int. J. Electrochem. Sci., 12 **(2017)** 7039 – 7047, doi: 10.20964/2017.08.73

International Journal of
ELECTROCHEMICAL
SCIENCE
www.electrochemsci.org

Short Communication

The Influence of Cl^- and Ca^{2+} on the Passive Film of 00Cr10MoV Steel in Simulated Concrete Solution

Jinyang Jiang[1,2,*], *Danqian Wang*[1,2], *Hong-yan Chu*[1,2], *Han Ma*[3] , *Jinjie Shi*[1,2], *Wei Sun*[1,2]

[1] School of Materials Science and Engineering, Southeast University, Nanjing 211189, China
[2] Jiangsu Key Laboratory of Construction Materials, Nanjing 211189, China
[3] Research Institute of Jiangsu Shasteel Iron and Steel, Zhangjiagang 215625, China
[*]E-mail: jiangjinyang16@163.com

Received: 22 March 2017 / *Accepted:* 12 June 2017 / *Published:* 12 July 2017

The influence of Cl^- and Ca^{2+} on the naturally growing passive film of a new, alloyed stainless steel with 10% Cr and 0% Ni was investigated by electrochemical impedance spectroscopy, Mott-Schottky curves, X-ray photoelectron spectroscopy (XPS), and transmission electron microscopy (TEM). The results showed that Ca^{2+} had an inhabitation effect on passive film dissolution and that Cl^- did not penetrate into the passive film, probably due to adsorption onto lower-energy oxygen vacancies and to the inhabitation effect of the space charge layer with a strong electric field. Local sites in the passive film thickened and the outer layer turned into an amorphous, porous structure due to its structural integrity. Additionally, the passive film remained passive in concrete.

Keywords: corrosion-resistant steel rebar; corrosion; passive films; TEM

1. INTRODUCTION

There are three stages for the pitting of metallic materials: (1) pitting nucleation, (2) metastable growth of the pit, and (3) stable pit growth. Many studies have made substantial progress by focusing on the micro-scale metastable growth and the stable pit growth [1]. However, the nano-scale passive breakdown of films continues to be debated, despite several investigations into it. The main controversies lie in the attack mechanism of chloride and the impact of chloride on the passive film. Two mechanisms of chloride are proposed, namely, absorption and penetration [2, 3], based on different film growth and breakdown conditions and different analytical techniques. However, the relationship between the adsorption mechanism and the penetration mechanism has not yet been discussed.

Cl^- could influence the composition, structure, and morphology of the passive film. The Fe and Cr content decreased due to the dissolution of the Fe-Cl complex [4]. Cl^- increased the roughness of the passive film surface [5]. So far, few reports have detailed a directly observed structure change in the passive film after the addition of Cl^-.

A simulated concrete solution is commonly used to simulate the concrete environment. Ghods reported that the pore solution composition has an effect on the protective properties of the passive oxide films and, in particular, sulfate ions $(SO_4)^{2-}$ have been shown to have a negative influence on the film quality [6]. Nevertheless, the effect of $Ca(OH)_2$, which the pore solution usually consists of, on the passive film was slightly investigated.

In this study, electrochemical impedance spectroscopy, X-ray photoelectron spectroscopy (XPS) and transmission electron microscopy (TEM) were used to investigate the relationship between the passive film of a new alloyed stainless steel rebar and the Cl^- and Ca^{2+} ion mechanism in high chloride alkaline concrete environments.

2. EXPERIMENTAL

2.1. Materials

00Cr10MoV is a new, alloyed corrosion-resistant steel that was designed to provide good corrosion resistance, reduce cost and enhance weldability in severe environments compared with duplex stainless steel. The moderate corrosion resistance was attributed to the effect of combining 10% Cr and 1% Mo and to an ultra-low carbon content, which lead to fewer inclusions.

The investigated samples were 10 mm-thick discs cut from a 16-mm diameter rod. The chemical composition of 00Cr10MoV steel is shown in Tab. 1.

Table 1. Chemical composition of 00Cr10MoV steel (wt%)

Steel	C	Si	Mn	Cr	Cu	Ni	Al	Mo
00Cr10MoV	0.01	0.487	1.49	10.36	-	-	-	1.162

After cutting to size, the samples were ground with progressively increasing grit sizes and then polished to 2.0 μm using diamond polish to eliminate the heterogeneities of the steel surface. The samples were then ultrasonically rinsed with distilled water, followed by ultrasonic cleaning in acetone to remove the surface contaminants, air dried and then used immediately for all the electrochemical corrosion experiments.

To study the passive and chloride-induced behaviour more systematically, the electrolyte used in this study was a representative concrete pore solution with 0.6 M KOH + 0.2 M NaOH + Sat. $Ca(OH)_2$ (pH 13.3). NaCl was added to the solution in incremental amounts until 5 M was reached after samples had been immersed in the simulated pore solution for 10 days. The time between each chloride addition was 24 h.

2.2. Electrochemical measurements

All the electrochemical tests were performed in a conventional three-electrode cell where the sample had 1 cm^2 exposed to the pore solution to serve as the working electrode. A saturated calomel electrode (SCE) acted as the reference electrode and was placed between the sample and the platinum plate. All potentials reported in this study are shown versus SCE. All the electrochemical measurements were carried out by a Princeton Parstat P4000 electrochemical system.

The electrochemical impedance spectroscopy (EIS) tests were performed using an applied AC signal amplitude of 10 mV RMS which showed no signs of non-linearity. The frequency range of the EIS was from 100 kHz to 0.01 Hz. The fitting of the EIS data was done by the ZSimpWin software.

2.3. Surface analysis

X-ray diffraction qualitative phase analysis was performed with a PHI Quantera SXM XPS system, using a monochromatized Al K X-ray source. The analysed area had a diameter of approximately 3 μm. Sputter depth profiles were measured for the passive films of the specimens using an argon gun of Ar^+ ions with a beam energy of 500 V and a beam current of 20 mA.

A cross section of the passive films after a 10-day passivation and a 30-day chloride induction was studied by STEM (Scanning Transmission Electron Microscope)/FIB (Focused Ion Beam). The STEM sample was prepared using a focused ion beam (FIB) system at an accelerating voltage of 30 kV, followed by a carbon deposition to protect the surface of the specimen [7, 8]. Transmission electron microscopy (TEM), high-angle annular dark-field scanning transmission electron microscopy (HAADF-STEM) and STEM energy-dispersive X-ray spectroscopy (HAADF-STEM-EDS) were conducted on an FEI Tecnai F20 transmission electron microscope at an acceleration voltage of 200 kV. EDS analyses were obtained in the scanning transmission electron microscopy (STEM) mode using a probe diameter of 1~2 nm.

3. RESULTS AND DISCUSSION

3.1. Electrochemical impedance spectroscopy (EIS) results

In this paper, EIS is used to monitor the corrosion behaviour of steel rebar in solutions with increasing chloride concentrations. Fig. 1 shows the EIS result of 00Cr10MoV steel rebar in Cl^-. The radius of the partial circle curves in the low frequency range of the Nyquist plot represent the polarization impedances of the passive films. The decreasing semicircle radius with increasing Cl^- concentration indicated a reduced impedance in the passive film, which was consistent with previous reports [9]. The Bode plot showed a broadening plateau in the middle frequency region, which indicated a stable passive state of steel with addition of Cl^- [10,11]. It should be noted that EIS is a macro-scale test method and thus the result is an average value. Therefore, micro-scale experiments were carried out with EIS tests.

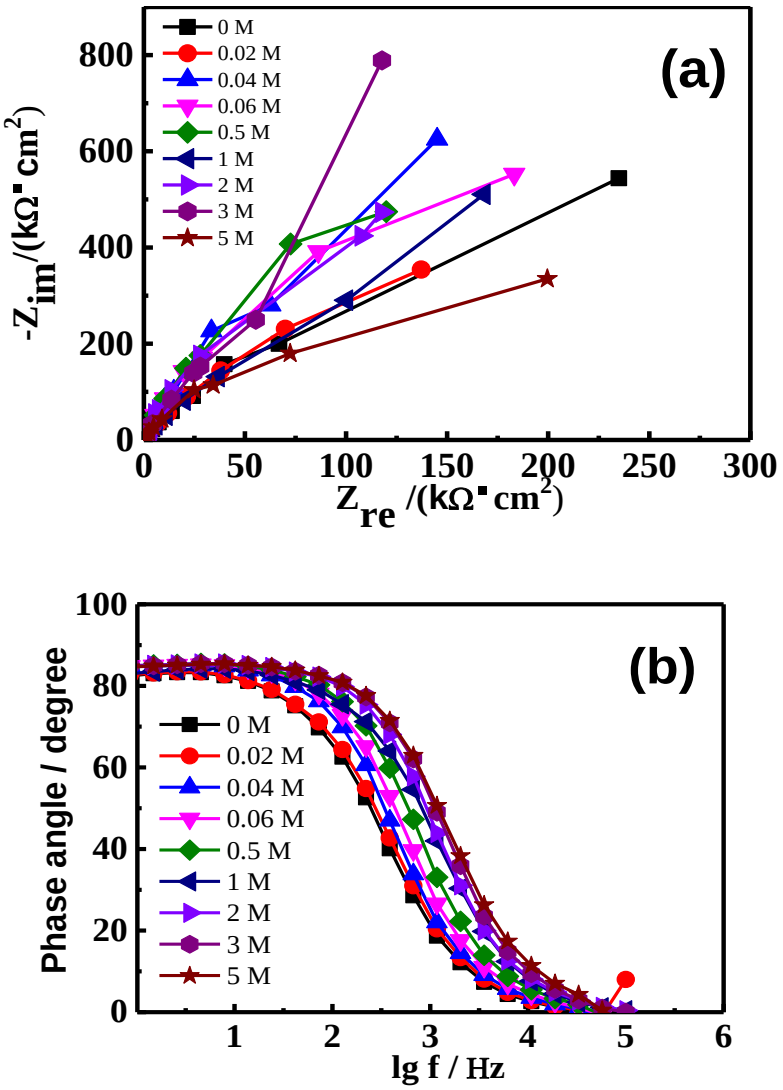

Figure 1. Electrochemical impedance spectrum of 00Cr10MoV steel specimens in different concentrations of Cl^-: (a) Nyquist; (b) Bode phase.

3.2. Cl^- and Ca^{2+} distribution in the passive film

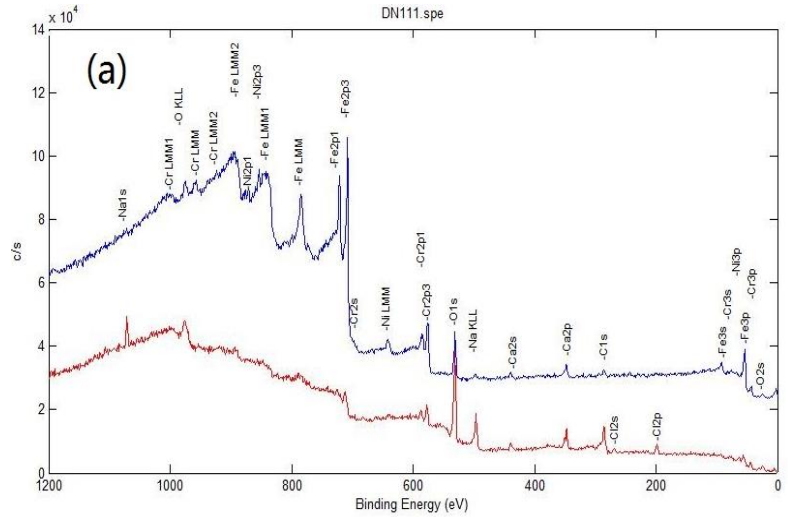

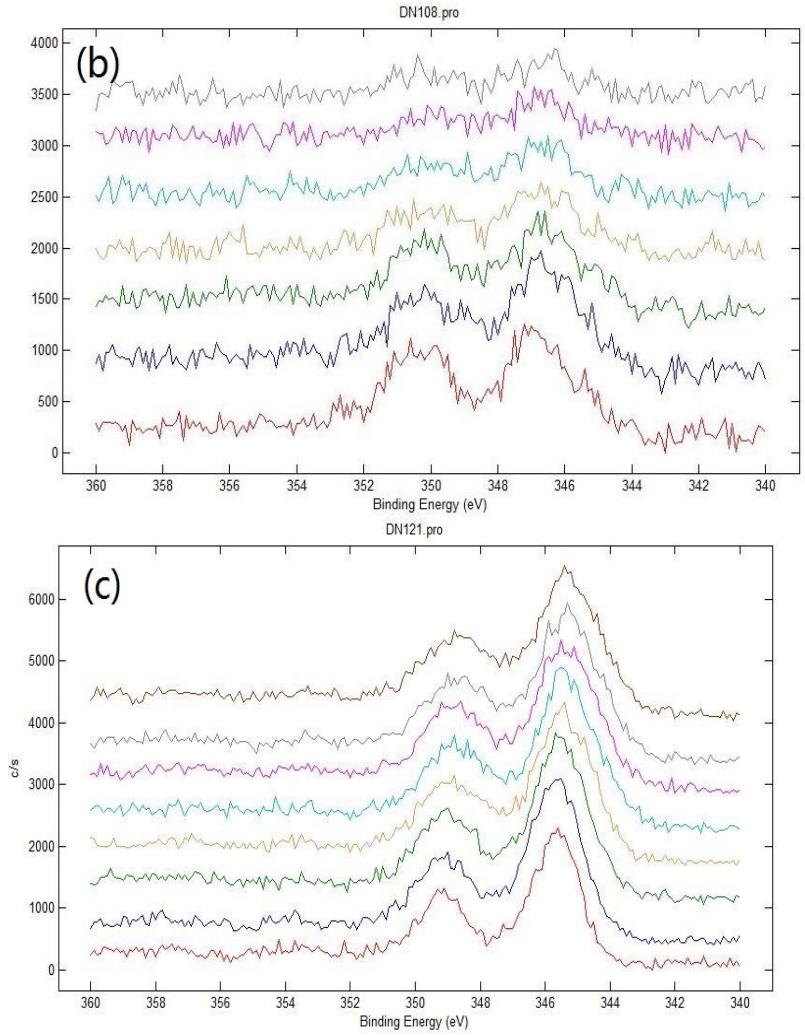

Figure 2. XPS spectrum of 00Cr10MoV steel specimens: (a) full spectrum from 0 nm and 3 nm (5 M Cl^-); (b) Ca XPS peak after pre-passivation; (c) Ca XPS peak (5 M Cl^-)

In addition to the compositional variations in the passive films of steel substrates that were reported by many studies [12-14], the presence of Ca and Cl from the external environment also plays an important role in the passive growth and breakdown processes. Fig. 2 shows the XPS spectrum of 00Cr10MoV steel specimens. The Cl^- peak only appeared on the surface of the passive film, according to Fig. 2a, which is consistent with previous studies investigating how the film naturally formed [15]. However, according to previous reports, chloride ions appeared in the passive film when an electric field, high temperatures or chloride ions were applied externally [15-17]. In this study, the concentration gradient was the only driving force for Cl^- transport. Obviously, this force could not overcome the resistance, inhibiting Cl^- penetration into the passive film. Cl^- probably could only adsorb onto the oxygen vacancies, which had lower energy, to form soluble complexes [18].

Ca peaks at various depths in the passive film are presented in Fig. 2b and 2c. Ca appeared in the outer passive film layer after pre-passivation. Ghods et al. explained the presence of Ca in the passive film by the adsorption of $Ca(OH)_2$ particles onto the steel surface [19]. There was probably no path for Ca to penetrate into the inner layer due to its high density.

Additionally, Ca peaks existed throughout the whole film when Cl^- was added. Unlike Cl^-, Ca^{2+} is positively charged. The positive charge of Ca^{2+} promoted its transport through the space charge layer, which had a strong electric field (on the order of 10^6 to 10^7 V/cm) [20] oriented from the outer layer to the inner layer. It could be deduced that the transport of the negatively charged Cl^- was inhibited by this electric field.

3.3. The influence of Cl^- and Ca^{2+} on the structure of passive film

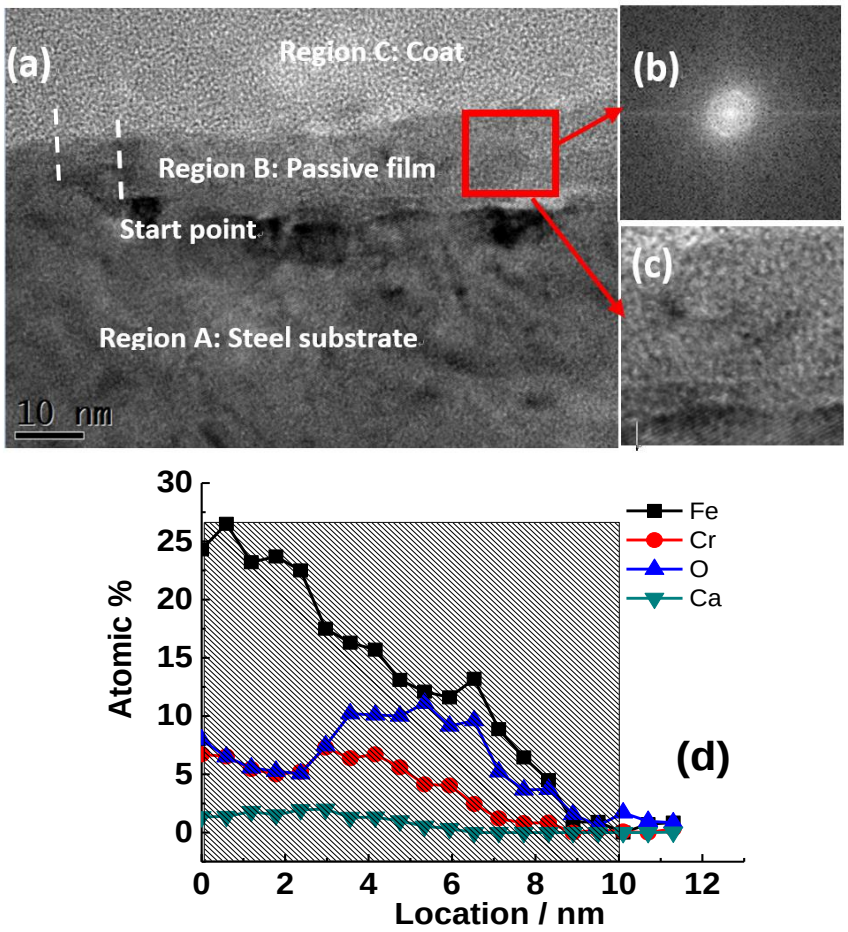

Figure 3. Thickness increase of the 00Cr10MoV steel passive film induced by chloride ([Cl^-]=5 M): (a) high resolution bright field image; (b) FFT image; (c) passive film interface magnified image; (d) EDS atomic distribution of the passive film.

Direct observation of the passive film was obtained by TEM. Fig. 3a and 4a show the high resolution TEM bright field image of the local passive film exposed in Cl^-. Regions A, B, and C represent a metal, a passive film, and a sputtered coat layer, respectively. In some areas, the passive film thickened to approximately 10 nm, as shown in Fig. 3a. The passive film became amorphous, according to e. 3b and 3c. Instead, a 5 nm-thick passive film that was still crystalized in the inner layer was formed, as shown in Fig. 4a, 4b and 4c.

The EDS results showed no evidence for Cl^- in the passive film, and the Ca content increased in the thickened passive film (Fig. 3d and Fig. 4d), which was consistent with the results from XPS.

According to previous reports, passive film remained the same, when [Cl^-] was below the critical chloride value [21], while thinning occurred when [Cl^-] was beyond the critical chloride value [21]. Few studies reported the thickening of the passive film with the addition of Cl^-. The probable reason for the thickening of the passive film in this study was the presence of Ca. Most likely, [Cl^-]=5 M was beyond the critical value and adsorbed onto enough oxygen vacancies on the passive film surface. Thus, according to Eq. (1) and (2) [22], ferrous ions dissolved into the solution.

$$Fe(\text{III}) + 2Cl^-(ads) \leftrightarrow [Fe(\text{II})Cl_2]_{surf} + 1e^- \quad (1)$$

$$[Fe(\text{II})Cl_{2]_{surf}} + h^+ + aq \rightarrow Fe^{3+}(aq) + 2Cl^-(aq) \quad (2)$$

$$Fe^{3+}(aq) + 3OH^-(aq) \leftrightarrow Fe(OH)_3(s) \quad (3)$$

The electromigration-dominated flux of cation vacancies increased from the barrier layer/outer layer interface to the metal/barrier interface [23]. As discussed above, Ca could occupy cation vacancies in the inner passive film layer, which allowed more cations at the steel/film interface to form a new passive film. Consequently, the cation growth rate outnumbered the dissolution rate, which led to the thickening of the passive film.

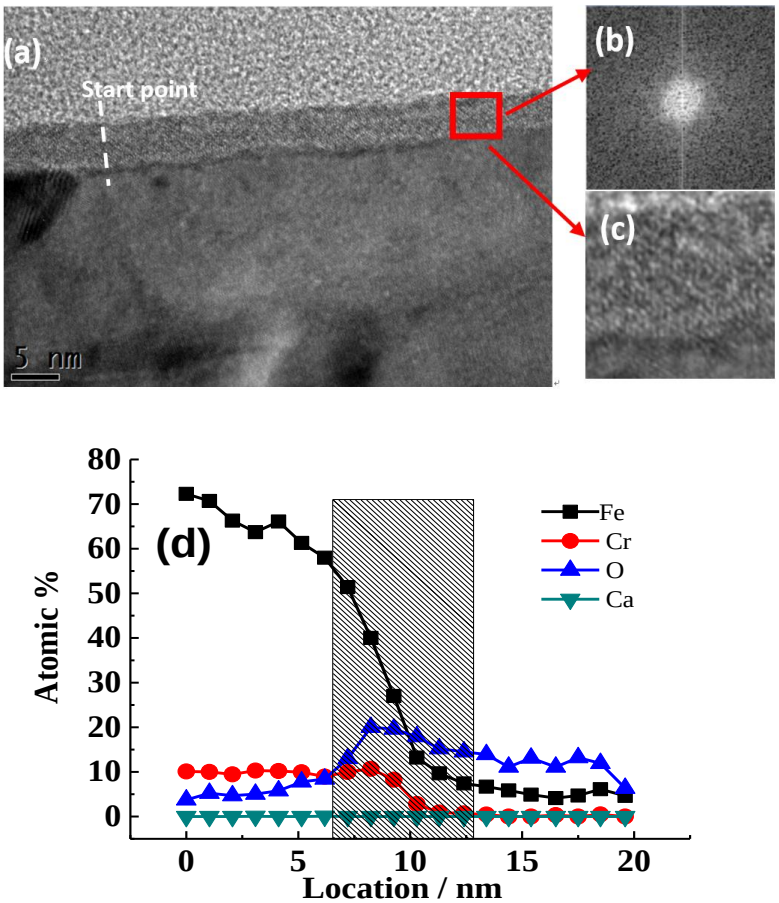

Figure 4. Homogeneous passive film of 00Cr10MoV steel specimens exposed to chloride ([Cl^-]=5 M): (a) high resolution bright field image; (b) FFT image; (c) passive film interface magnified image; (d) EDS atomic distribution of the passive film.

Since Cl^- only adsorbed on the locally defective passive film surface, only the outer layer dissolved. New cations from the metal/passive film interface reacted with OH^- in solution to form a new outer layer. Therefore, the lattice structure of the defective part of the outer passive film layer changed into an amorphous structure due to a higher film growth rate. There was limited time for the vacancies/atoms/ions to diffuse to their proper positions, which generated more defects in the passive film and thus increased the carrier densities. However, the number of cation vacancies only changed in the inner passive film layer, and thus the lattice structure did not change. Since the integrity of the passive film structure was maintained, the space charge layer under a strong electric field still ensured a high corrosion resistance in the passive film. Therefore, the macro-scale electrochemical behaviour showed no corrosion, as shown in Fig. 1. However, the amorphous structure of outer layer led to a more defective film which was more sensitive to corrosion [24].

5. CONCLUSION

(1) Due to the lower energy of oxygen vacancies on some defective sites on the passive film surface and the inhabitation effect of the space charge layer with strong electric fields, Cl^- only absorbed onto the passive film surface.

(2) Ca^{2+} filled the cation vacancies in the inner passive film layer, inhibiting the dissolution of the inner layer and promoting the growth of outer layer.

(3) Although the macro-scale showed no corrosion on the steel rebar, local sites on the passive film thickened and changed into an amorphous structure after the addition of Cl^-, revealing a sensitivity to corrosion.

ACKNOWLEDGEMENTS
The authors acknowledge support by the National Natural Science Foundation of China (Nos. 51278098 and 51678144), the National Basic Research Program of China "973 Project" (No. 2015CB655100) and the Industry-University Research Cooperative Innovation Fund of Jiangsu Province (No. BY2013091).

References

1. G. S. Frankel, L. Stockert, F. Hunkeler, and H. Boehni, *Corrosion*, 43(7) (1987) 429.
2. Y. F. Cheng, and J. Y. Luo, *Appl Surf Sci*, 167 (2000) 113.
3. P. Marcus, V. Maurice, and H-H. Sterhblow, *Corros Sci*, 50 (2008) 2698.
4. T-O. Benoit, A-D. Catherine, and B. Normand, *Electrochim Acta*, 133 (2014) 373.
5. C. M. Abreu, M. J. Cristobal, and R. Losada, *Electrochim Acta*, 51(8) (2006) 1881.
6. P. Ghods, O. B. Isgor, G. Mcrae, and T. Miller, *Cem Concr Compos*, 31(1) (2009) 2.
7. J. Sikora, E. Sikora, and D. D. Macdonald, *Electrochem Acta*, 45 (2000) 1875.
8. T. Dan, T. Shoji, Z. Lu, K. Sakaguchi, J. Wang, E-H. Han, and W. Ke, *Corros Sci*, 52 (2010) 1228.
9. Lv J, H. Luo, *J. Nucl. Mater.*, 452(1) (2014) 469.
10. K.R. Trethewey, M. Paton, *Mater. Lett.*, 58(27) (2004) 3381.
11. M. Chembath, J.N. Balaraju, M. Sujata, *Mater. Sci. Eng., C*, 56 (2015) 417.

12. J. Hogstrom, W. Fredriksson, K. Edstrom, F. Bjorefors, L. Nyholm, and C-O. A. Olsson, *Appl Surf Sci*, 284 (2013) 700.
13. A. Bautista, G. Blanco, F. Velasco, A. Gutierrez, L. Soriano, F. J. Palomares, and H. Takenouti, *Corros Sci*, 51(4) (2009) 785.
14. W. Fredriksson, and S. Malmgren, *Appl Surf Sci*, 258(15) (2012) 5790.
15. C. Hubschmid, and D. Landolt, *J Electrochem Soc*, 140(7) (1993) 1898.
16. W. P. Yang, D. Costa, and P. Marcus, *J Electrochem Soc*, 141(10) (1994) 2669.
17. S. Mischler, A. Vogel, H. J. Mathieu, and D. Landolt, *Corros Sci*, 32(9) (1991) 925.
18. P. Marcus, V. Maurice, and H-H. Strehblow, *Corros Sci*, 50(9) (2008) 2698.
19. G. Pouria, Multi-scale investigation of the formation and breakdown of passive films on carbon steel rebar in concrete. Diss. Carleton University Ottawa, USA, 2010.
20. G. S. Frankel, *Electrochem Soc*, 145(6) (1998) 2186.
21. S. Fajardo, D. M. Bastidas, M. P. Ryan, M. Criado, D. S. Mcphail, R. J. H. Morris, and J. M. Bastidas, *Appl Surf Sci*, 288 (2014) 423.
22. I. Diez-Perez, C. Vericat, P. Gorostiza, and F. Sanz, *Electrochem Commun*, 8(4) (2006) 627.
23. A. Veluchamy, D. Sherwood, B. Emmanuel, and I. S. Code, *J Electroanal Chem*, 785 (2017) 196.
24. A. Poursaee, *Electrochem Commun*, 73 (2016) 24.